

# Oxidative stress induces tau hyperphosphorylation via MARK activation in neuroblastoma N1E-115 cells

Yuhong Liu,<sup>1</sup> Yunxi Chen,<sup>2</sup> and Koji Fukui<sup>1,2,\*</sup>

<sup>1</sup>Molecular Cell Biology Laboratory, Department of Functional Control Systems, Graduate School of Engineering and Science and <sup>2</sup>Molecular Cell Biology Laboratory, Department of Systems Engineering and Science, School of Engineering and Science, Shibaura Institute of Technology, Fukasaku 307, Minuma-ku, Saitama 337-8570, Japan

(Received 29 March, 2022; Accepted 28 December, 2022; Released online in J-STAGE as advance publication 16 May, 2023)

Reactive oxygen species are considered a cause of neuronal cell death in Alzheimer's disease (AD). Abnormal tau phosphorylation is a proven pathological hallmark of AD. Microtubule affinity-regulating kinases (MARKs) regulate tau-microtubule binding and play a crucial role in neuronal survival. In this study, we hypothesized that oxidative stress increases the phosphorylation of Ser262 of tau protein through activation of MARKs, which is the main reason for the development of AD. We investigated the relationship between tau hyperphosphorylation on Ser262 and MARKs in N1E-115 cells subjected to oxidative stress by exposure to a low concentration of hydrogen peroxide. This work builds on the observation that hyperphosphorylation of tau is significantly increased by oxidative stress. MARKs activation correlated with tau hyperphosphorylation at Ser262, a site that is essential to maintain microtubule stability and is the initial phosphorylation site in AD. These results indicated that MARKs inhibitors might serve a role as therapeutic tools for the treatment of AD.

**Key Words:** tau phosphorylation, Alzheimer's disease, microtubule affinity-regulating kinases, oxidative stress, microtubule-associated proteins

In 1956, Denham Harman proposed that aging and age-related diseases might result from the effects of free radical damage, which he called the free radical theory of aging. Free radical diseases include Alzheimer's disease (AD), Parkinson's disease (PD), and other neurodegenerative disorders.<sup>(1)</sup> Free radicals are generated as a consequence of ATP production in the mitochondrial electron transport chain. Overproduction of free radicals induces imbalance of redox status and may result in deleterious effects on the cell membranes proteins, lipids, lipoproteins, and DNA.<sup>(2,3)</sup> Hydrogen peroxide (H<sub>2</sub>O<sub>2</sub>) is one of the reactive oxygen species (ROS) and is well-known as a normal metabolite of oxygen in the aerobic metabolism of organisms which was first shown in 1970 by detected catalase Compound I in the intact perfused liver.<sup>(4)</sup> Some transition metals like Fe<sup>2+</sup> can break down hydrogen peroxide into the reactive hydroxyl radical which is one type of free radical by the Fenton reaction.<sup>(5)</sup> Therefore, H<sub>2</sub>O<sub>2</sub> is considered an effective simulation of the oxidative stress model.

The human brain consumes around 20% of the body's oxygen supply, meaning that the brain suffers greater exposure to oxidative stress as a result of this high level of energy consumption. Therefore, it is reasonable to conjecture that neurons are more vulnerable to oxidative stress.<sup>(6)</sup> Oxidative stress, which attacks nerve cells and induces cell death, is one reason for the development of AD. The brain is especially vulnerable to such damage

because the regeneration of the nerve cell network is extremely difficult. Avoidance of AD clearly requires the prevention of neuronal cell death, and such prophylaxis necessitates clarification of the signs of neuronal degeneration that precede cell death.<sup>(7)</sup>

Accumulation of the peptide amyloid- $\beta$  (A $\beta$ ) and formation of intracellular neurofibrillary tangles (NFTs) are two hallmarks of AD. A $\beta$  has been believed to play the most important role in AD pathogenesis for a very long time. The A $\beta$  hypothesis says the accumulation of A $\beta$  plaques extracellularly leads to severe dementia associated with AD.<sup>(8)</sup> However, many clinical trials show that potential strategies targeting A $\beta$  failed. It may be due to targeting A $\beta$  only having beneficial effects during the early stages before cognitive impairments of the disease.<sup>(9,10)</sup> On the contrary, there are some researchers who indicated that the level of NFTs pathology has a positive correlation with the cognitive state in AD patient's brain before autopsy.<sup>(11)</sup> Taken together, more and more researchers suggest that tau pathology is more potential to be a strategy for drug investigation of AD.

Tau, an unfolded highly soluble protein, is one kind of microtubule-associated protein (MAP), and plays an important role in microtubule stabilization for maintenance of basal neuronal functions.<sup>(12)</sup> In AD brains, tau hyperphosphorylation is believed to be a key factor that affects microtubule assembly and induces tau aggregation. Conversion of tau from a monomer form to an oligomer induces aggregation via the formation of paired helical filaments (PHFs), leading in turn to the formation of NFTs, a hallmark of the brains of patients with AD.<sup>(13)</sup> Multiple studies have shown that tau proteins bind to microtubules and strongly affect axonal transport.<sup>(14,15)</sup> The tau protein harbors several phosphorylation sites, including Ser262, and Ser356, which correspond (respectively) to the first and fourth KXGS motifs within the tubulin-binding domain. Phosphorylation at these sites has been reported to inhibit the binding of normal tau to microtubules, thereby leading to the disruption of microtubule assembly.<sup>(16)</sup> Members of the Ser/Thr protein kinase family include proteinase-activated receptor 1 (PAR-1), protein kinase in *S. cerevisiae* (KIN1) and microtubule affinity-regulating kinases (MARKs). Many of these kinases have been shown to contribute to the regulation of microtubule stability, protein stability, intracellular signaling, and cell division, and additionally have been implicated in AD.<sup>(17)</sup>

The MARK family consists of 4 proteins, including MARK1, MARK2 (EMK1), MARK3 (C-TAK1), and MARK4 (MARKL-1).

\*To whom correspondence should be addressed.  
E-mail: [koji@sic.shibaura-it.ac.jp](mailto:koji@sic.shibaura-it.ac.jp)

The activation of MARKs is regulated by multiple mechanisms, including phosphorylation at a threonine residue (T215 in MARK1, T208 in MARK2, T211 in MARK3, and T214 in MARK4) in the activation loop (also referred to as the T-loop) by upstream kinases such as liver kinase B1 (LKB1) and MARK kinase (MARKK).<sup>(18)</sup> Other work has shown that glycogen synthase kinase 3 $\beta$  (GSK3 $\beta$ ) inhibits MARK activity by phosphorylating a serine residue (S219 in MARK1, S212 in MARK2, S215 in MARK3, and S218 in MARK4), impeding the ability of these Ser residues to interact with the amino acids in the T-loop of their target.<sup>(19)</sup> Multiple studies have reported that MARKs phosphorylate MAPs at the microtubule-binding domain, thereby disrupting the binding of MAPs to microtubules and changing microtubule dynamics.<sup>(17,20)</sup> Serine 262 is a major serine site in tau that is specifically phosphorylated by MARKs. This residue has been found to be hyperphosphorylated in tau isolated from the NFTs in brains of AD patients. In addition, tau purified from NFTs appears to have lost the ability to bind microtubules.<sup>(21)</sup> Several researchers have reported the hyperphosphorylation of tau in the brains of patients with AD, suggesting that phosphorylation of tau at Ser262 is an early pathological change in the course of AD that leads in turn to the abnormal further accumulation of tau.<sup>(22–25)</sup> Prevention of tau phosphorylation at Ser262 has been reported to reduce tau toxicity and retard tau-induced neurodegeneration in cultured cells and mouse models.<sup>(26–30)</sup> Taken together, these results suggest that oxidative stress is an instigator of the onset of AD, and would result from activation of the MARKs signaling pathway, such that MARKs activation would lead to phosphorylation of tau at the Ser262 site. Several previous studies have shown that exposure of neuronal cells to a low concentration of hydrogen peroxide induces axonal degeneration, leading in turn to abnormal morphologies, including shrinkage, fragmentation, and beading of neurites. Those abnormal morphologies are markers of axonal degeneration, and are known to precede neural cell death.<sup>(7)</sup>

N1E-115 cells, which are derived from a neuroblastoma, are undifferentiated cells that normally do not elongate neurites. The interaction of cells with extracellular matrix (ECM) protein is mediated by integrins, which act as cell surface receptors composed of heterodimers of  $\alpha$  and  $\beta$  subunits.<sup>(31)</sup> There are many different intracellular pathways when integrins bind the ECM ligands in different types of cells. They differ depending on specific ECM ligand interactions and specific intracellular signaling protein. In neuronal cells, the formation of neurites is one of the responses of differentiation which can be promoted by ECM ligands such as laminin, fibronectin, or collagen.<sup>(32)</sup> In addition, it has been reported that N1E-115 cells exhibit neurite outgrowth in response to serum deprivation can be enhanced when the cells are grown on a laminin matrix.<sup>(33)</sup> N1E-115 cells, compared with other types of neuronal cells such as PC12 cells which require growth factors to enhance neurite outgrowth such as nerve growth factor (NGF) are a more efficient model for AD study. However, there is no evidence showing the MARKs expression in N1E-115 cells.

In the present study, we investigated the connection between tau hyperphosphorylation and MARKs activity. Specifically, we showed that exposure of the N1E-115 cell line to a low concentration of hydrogen peroxide induced oxidative stress, resulting in changes in the balance between phosphorylated and unphosphorylated MARKs and leading to hyperphosphorylation of tau at Ser262.

## Materials and Methods

**Cell culture.** N1E-115 cells (ECACC #88112303) were obtained from Sumitomo Dainippon Pharma Corp., Ltd. (Osaka, Japan). This cell line is derived from a mouse neuroblastoma C1300 tumor. N1E-115 cells were incubated at 37°C in a 5%

CO<sub>2</sub> environment, and were grown in Dulbecco's minimum essential medium (D-MEM-Low glucose) containing Phenol Red (FUJIFILM Wako Pure Chemical Corp., Osaka, Japan) supplemented with 5% heat-inactivated fetal bovine serum (FBS; Biological Industries, Kibbutz Beit Haemek, Israel), 6  $\mu$ M L-glutamine (FUJIFILM Wako Pure Chemical Corp.), 50 U/ml penicillin, and 50 mg/ml streptomycin. N1E-115 cells were plated in 100-mm dishes. After 24 h of growth, N1E-115 cells were trypsinized, re-suspended in conditioned serum-free medium, and plated in 35-mm dishes at a density of  $4 \times 10^4$  cells/ml or in 24-well plates at a density of  $2 \times 10^4$  cells/ml. These dishes or plates previously had been double-coated with 0.2% polyethyleneimine (PEI) and 10  $\mu$ g/ml mouse laminin which derived from mouse Engelbreth-Holm-Swarm (EHS) sarcoma (FUJIFILM Wako Pure Chemical Corp.) to facilitate cell growth. After 24 h, the medium was replaced with conditioned serum-free medium supplemented with 1% dimethyl sulfoxide (DMSO). After a further 48-h incubation, the resulting cells were used for experiments. Conditioned medium was obtained from 48-h cultures of N1E-115 cells grown to 80–90% confluence in serum-free complete medium (prepared as above but lacking FBS) supplemented with 1% DMSO. DMSO was used here to elicit neurite elongation.

**Optimization of hydrogen peroxide concentration.** The optimal hydrogen peroxide concentration was determined empirically. N1E-115 cell survival was evaluated by the trypan blue dye exclusion assay. After confirming neurite elongation, cells (growing in 35-mm dishes) were exposed to a range of hydrogen peroxide (FUJIFILM Wako Pure Chemical Corp.) concentrations (0, 1, 5, 10, 20, and 50  $\mu$ M) for 24 h; hydrogen peroxide was added to each dish at a final concentration of 0.8% (w/v). Trypan blue staining solution [diluted with phosphate-buffered saline (PBS) to a final concentration of 0.4%] was added to each dish, and the dishes were incubated in a CO<sub>2</sub> incubator at 37°C for 20 min. Following this incubation, the cells were washed at least three times with PBS. Photomicrographs of the cells were recorded using an Olympus IX81 phase-contrast microscope (Olympus Corp., Tokyo, Japan) that was equipped with an Olympus DP71 digital camera (Olympus Corp.). Analysis was performed by selecting random fields from photomicrographs of cells exposed to each concentration of hydrogen peroxide. The number of living cells and the total number of cells were counted from each randomly selected field. The number of dead cells then was expressed as a percentage normalized to the total cell number. At least three dishes were analyzed for each concentration of hydrogen peroxide, and each experiment was repeated three times. To ensure objectivity, counts were performed independently by personnel not involved in the present study.

**Immunocytochemical analysis.** To examine the localization of MARKs in N1E-115 cells, immunostaining was performed. The cells were grown on glass coverslips and exposed to 5 and 10  $\mu$ M hydrogen peroxide for 24 h following the induction of neurite elongation. Following exposure, the cells were washed at least three times with PBS, then fixed with 4% paraformaldehyde (PFA; Merck Millipore, Darmstadt, Germany) in PBS for 15 min at 4°C. The fixed cells were blocked for 1 h at room temperature (RT) with a blocking solution consisting of PBS containing 10% goat serum and 0.3% Triton X-100. The cells were probed by incubation overnight at 4°C with dilutions of each primary antibody [anti-TAU-5, #ab80579; anti-Tau phospho S262, #ab131354; anti-MARK 1+2+3+4, #ab74131; and anti-MARK4 (phospho T214) + MARK2 (phospho T208) + MARK3 (phospho T234) + MARK1 antibody (EPR5463), #ab126731]. All of these antibodies were obtained from abcam plc., and were diluted in an antibody dilution buffer consisting of PBS containing 1% bovine serum albumin (BSA), 1% normal goat serum (Agilent Technologies, Santa Clara, CA) and 0.3% Triton X-100. The cells then were

incubated for 2 h at 4°C with Alexa Fluor 488 green (Thermo Fisher Scientific, Inc.)-conjugated F(ab')<sub>2</sub>-fragment of goat anti-mouse immunoglobulin G (IgG) (H + L) or Alexa Fluor 488 green-conjugated F(ab')<sub>2</sub>-fragment of goat anti-rabbit IgG (H + L). These secondary antibodies were diluted 1:150 in antibody dilution buffer solution. The cells were counterstained at 4°C for 20 min with Hoechst 33258 (FUJIFILM Wako Pure Chemical Corp.) and then mounted on slide glasses. Photomicrographs of fluorescently labeled cells were recorded using phase-contrast on a fluorescence microscope equipped with a digital camera. At least three wells were analyzed for each experimental group, cells for analysis were selected randomly among each group and each run was repeated for a total of three independent experiments. The fluorescence brightness relative ratios of labeling for MARKs and pMARKs were calculated by dividing the relative brightness value for each hydrogen peroxide-exposed group by that of the control group. This analysis was performed using Image-J software (National Institutes of Health, Bethesda, MD).

**Western blotting.** N1E-115 cells were harvested in lysis buffer following growth in DMEM containing 5% FBS. Sample lysates were centrifuged, and the protein content of the resulting supernatant was determined using a Bradford assay employing the Bio-Rad Protein Assay Dye Reagent Concentrate (#5000006; Bio-Rad Laboratories, Inc., Hercules, CA) according to the manufacturer's protocol. Aliquots containing consistent amounts (20 µg) of total protein were separated on a 12% sodium dodecyl sulfate (SDS)-polyacrylamide gel and transferred to a ClearTrans Nitrocellulose Membrane, 0.2 µm (FUJIFILM Wako Pure Chemical Corp.). Following transfer, the membranes were stained for 5 min with Ponceau S (Sigma Aldrich Corp., Merck KGaA, Darmstadt, Germany). The Ponceau S-stained membranes then were washed with TBST [Tris-HCl-buffered saline (TBS), pH 7.6, containing 0.1% Tween 20 and 2% non-fat skim milk], blocked for 1 h at RT with blocking solution (TBST containing 2% non-fat skim milk), and washed again with TBST. Membranes then were exposed overnight at 4°C to each of the primary antibodies [mouse monoclonal anti-TAU-5 antibody, 1:2,000, #ab80579; rabbit polyclonal anti-Tau (phospho S262) antibody, 1:2,000, #ab131354; rabbit polyclonal anti-MARK 1+2+3+4 antibody, 1:1,000, #ab74131; rabbit monoclonal anti-MARK4 (phospho T214) + MARK2 (phospho T208) + MARK3 (phospho T234) + MARK1 antibody (EPR5463), 1:2,000, #ab126731; and mouse monoclonal anti-β-actin antibody, 1:4,000, #ab8226]. All of these antibodies were obtained from abcam plc. Horseradish peroxidase (HRP)-conjugated anti-rabbit IgG antibody (#W4011, Promega Corp., Madison, WI) was used as a secondary antibody for anti-Tau (phospho S262) and anti-MARK4 (phospho T214) + MARK2 (phospho T208) + MARK3 (phospho T234) + MARK1 antibody (EPR5463)-reacted membranes; HRP-conjugated anti-mouse IgG antibody (#W4011, Promega Corp.) was used as a secondary antibody for anti-TAU-5 antibody, anti-MARK 1+2+3+4 antibody, and anti-β-actin antibody-reacted membranes. Specifically, membranes were incubated for 1 h at RT with a 1:4,000 dilution of the indicated secondary antibody. Each study was performed as a minimum of three independent experiments. Chemiluminescent signals were generated by reacting with enhanced chemiluminescence (ECL) reagents (Millipore, Bedford, MA), and signal intensities were detected using the LAS-3000 Image Reader (FUJIFILM Corp., Tokyo, Japan). Band intensities were normalized to that of the Ponceau S staining for the respective lane. This analysis was performed using ImageQuant TL 8.1 software (GE Healthcare Life Sciences, Tokyo, Japan).

**Statistical analysis.** ImageQuant TL 8.1 software was used for signal intensity analysis for Western blotting. Image-J software was used for cell fluorescence brightness analysis. Data were analyzed using Prism (ver. 6.02; GraphPad Software,

San Diego, CA) and JMP pro.16 (SAS Institute Japan Co., Ltd., Tokyo, Japan). Data were plotted as the mean ± SD of the results of at least three independent experiments. Data from two groups were compared using a two-tailed non-paired Student's *t* test. Data from three or more groups were compared using a two-tailed one-way analysis of variance (ANOVA) with post hoc Tukey-Kramer test. Values of *p* < 0.05 were considered significant.

## Results

**Neurite outgrowth and optimization of hydrogen peroxide concentration.** For this study, assessment of neurite morphology under oxidative stress conditions was required. Therefore, neurite outgrowth from N1E-115 cells was induced by serum withdrawal combined with exposure to 1% DMSO grown on a laminin matrix for 72 h (see Methods; Fig. 1A). The aim of this part of the study was to identify early signs of cell degeneration that occur following hydrogen peroxide exposure but prior to cell death. For this purpose, we focused on changes in neurite morphology. Cells were exposed to various concentrations of hydrogen peroxide (1, 5, 10, 20, and 50 µM) to induce oxidative stress, and then neurite degeneration (e.g., induction of beading) was evaluated. We observed that exposure to hydrogen peroxide induced cell death in an apparently concentration-dependent manner. The proportion of cell death was significantly elevated compared to the control group when the concentration of hydrogen peroxide was 10 µM or higher. In contrast, few changes in neurite morphology were observed at a hydrogen peroxide concentration of 1 µM (Fig. 1C). Therefore, 5 and 10 µM hydrogen peroxide were selected as the optimal concentrations for use in subsequent experiments.

**Localization of tau and phospho-tau (S262) in N1E-115 cells.** Tau is a type of MAP that interacts with the microtubules of the cellular cytoskeleton. Tau typically distributed throughout cell bodies and neurites. Given that morphological changes were observed on the neurites after exposure to 5 and 10 µM hydrogen peroxide, we investigated distribution of tau in the altered neurites. As expected, tau was present in both the cell bodies and neurites of control cells (Fig. 2A). Notably, tau remained detectable both in the cell bodies and degenerating neurites following exposure to 5 and 10 µM hydrogen peroxide. Similarly, it was confirmed that phospho-tau (S262) localizes to both cell bodies and neurites, both in control and hydrogen peroxide-exposed cells (Fig. 2B). However, in this study, there was no localization difference between phospho-tau and tau after treatment with hydrogen peroxide.

**Oxidative stress induces phosphorylation of tau at Ser262.** To clarify the relationship between tau and oxidative stress, we assessed tau protein levels by Western blotting. Tau protein levels were nominally (but not significantly) decreased in hydrogen peroxide-exposed cells compared to controls (ns; Fig. 3A). However, phospho-tau (Ser262) levels were significantly increased in the hydrogen peroxide-exposed cells compared to controls (*p* < 0.001; Fig. 3A). These data demonstrated that tau hyperphosphorylation correlate with oxidative stress.

**Increased Tau phosphorylation at Ser262 correlates with increased phosphorylation of MARKs under oxidative stress.** To determine the relationship between tau phosphorylation on Ser262 and MARKs activation, we assessed the protein levels of MARKs, pMARKs, tau and pTau by Western blotting. Phospho-MARKs levels were significantly increased in the hydrogen peroxide-exposed cells compared to the controls (*p* < 0.01; Fig. 3C). However, MARKs and tau levels did not show the difference in hydrogen peroxide-exposed cells compared to the controls (ns; Fig. 3C). Accordingly, these results indicated that the nominal decrease in tau protein level did not correlate with the protein levels of MARKs. Moreover, our data show

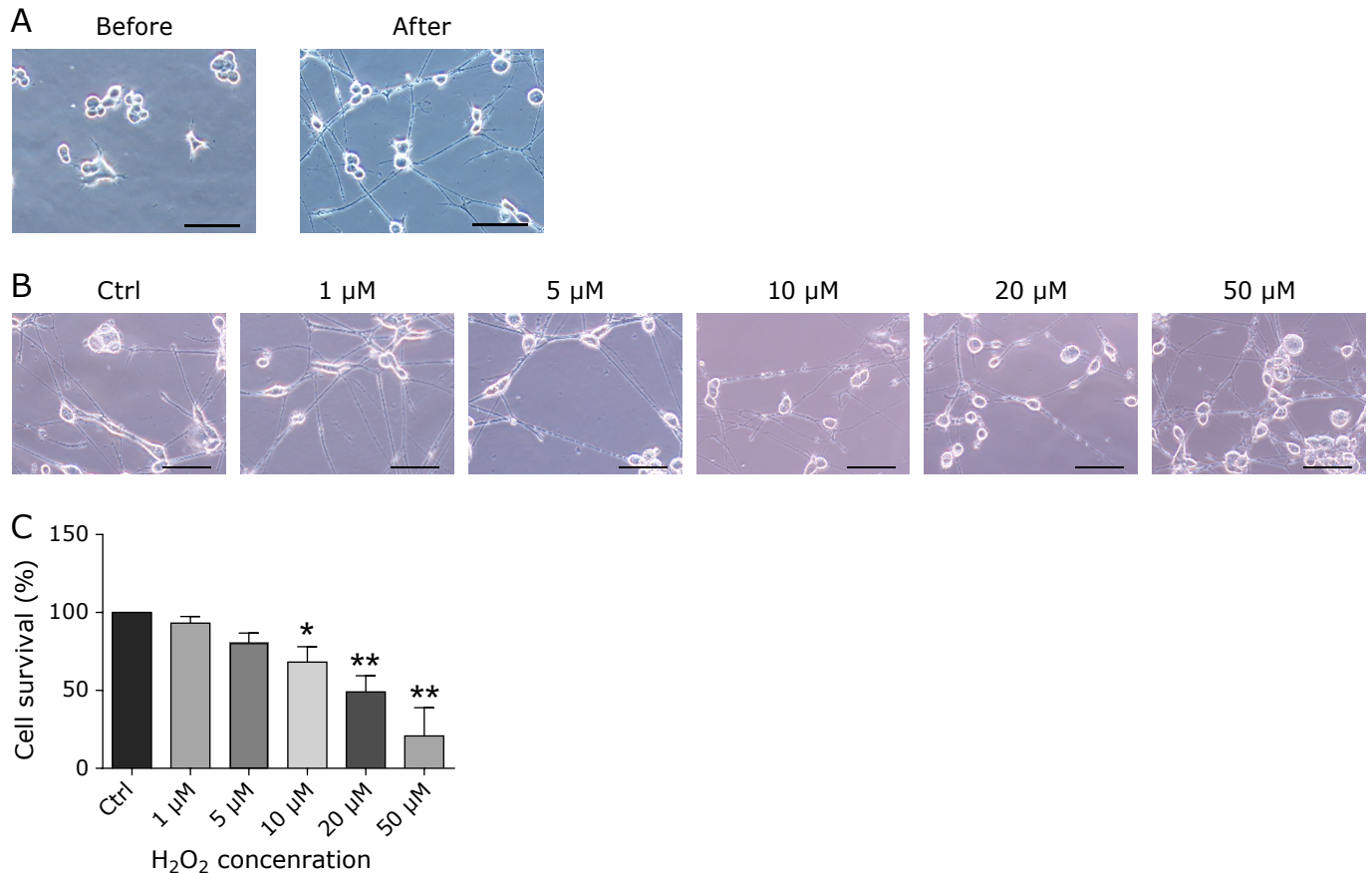


**Fig. 1.** Neurite elongation and effects of hydrogen peroxide exposure. (A) Morphology of neurite elongation before and after exposure of N1E-115 cells to 1% dimethyl sulfoxide solution (DMSO). (B) Induction of neurite degeneration in N1E-115 cells following exposure to various concentrations of hydrogen peroxide. Ctrl, control. Scale bars in both (A) and (B) are 100 μM. (C) Cell survival following exposure to various concentrations of hydrogen peroxide were assessed using trypan blue staining. Hydrogen peroxide induced cell death in an apparently concentration-dependent manner in N1E-115 cells. Survival in the control group (unexposed to peroxide) was defined as 100%. Data are plotted as mean + SD of at least three independent experiments. \* $p < 0.05$ , \*\* $p < 0.01$  (two-tailed one-way ANOVA with post hoc Tukey–Kramer's tests). See color figure in the on-line version.

that tau hyperphosphorylation on Ser262 under oxidative stress may correlates with the phosphorylation of MARKs.

**Immunocytochemical analysis shows that MARK phosphorylation is increased in hydrogen peroxide-exposed N1E-115 cells.** As noted above, the data from Western blotting show a significant difference in MARKs phosphorylation between hydrogen peroxide-exposed and control cells (Fig. 3C). To more accurately determine the phosphorylation of MARKs in hydrogen peroxide-exposed cells, we analyzed the relative ratios of cell brightness using an immunocytochemical assay (Fig. 4A). As expected, the results of Western blotting and immunocytochemistry show no significant difference in MARKs between hydrogen peroxide-exposed and control cells (Fig. 4B). In addition, phosphorylated MARKs have been stained and analyzed by the same method as MARKs (Fig. 5A). As we predicted, the levels of phosphorylated MARKs (pMARKs), were significantly increased in the hydrogen peroxide-treated cells compared to the controls (Fig. 5B). The ratio was assessed as a contrast to the pMARKs in exposed cells with control cells. Considered together, these data (derived from Western blotting and immunocytochemistry) demonstrated that MARKs phosphorylation correlates with tau hyperphosphorylation at Ser262 site.

## Discussion

**Hydrogen peroxide induces neurite degeneration before cell death of N1E-115 cells.** Free radicals in living organisms generally are divided into ROS and reactive nitrogen species (RNS); both are generated from cellular reduction/oxidation (redox) processes. The most common source of free radicals in biological systems is oxygen. Oxygen intermediates, including H<sub>2</sub>O<sub>2</sub>, the hydroxyl radical (HO•) and superoxide (O<sub>2</sub><sup>•-</sup>), are produced during cellular respiration. Both the hydroxyl radical and superoxide are free radicals, harboring a free electron in an outer orbit. Hydrogen peroxide is not a free radical but readily generates free radicals by reactions with other molecules in living tissues. Thus, hydrogen peroxide generally is considered an oxidant.<sup>(34)</sup> Very low concentrations of hydrogen peroxide are produced in the body and normally are detoxified by catalase or glutathione peroxidase. In the presence of iron ions, hydrogen peroxide produces hydroxyl radicals via the Fenton reaction. The hydroxyl radical is more reactive than other ROS and primarily attacks lipids, with the attacked lipids becoming lipid alkoxyl radicals.<sup>(5,35)</sup> In our experimental model, cultured neurons were exposed to very low concentrations of hydrogen peroxide. The concentration of hydroxyl radicals in spent medium produced by hydrogen peroxide-exposed cells has not been measured, but we expect that a low level of hydroxyl radicals was generated even in our experimental model. Therefore, to create an oxidative

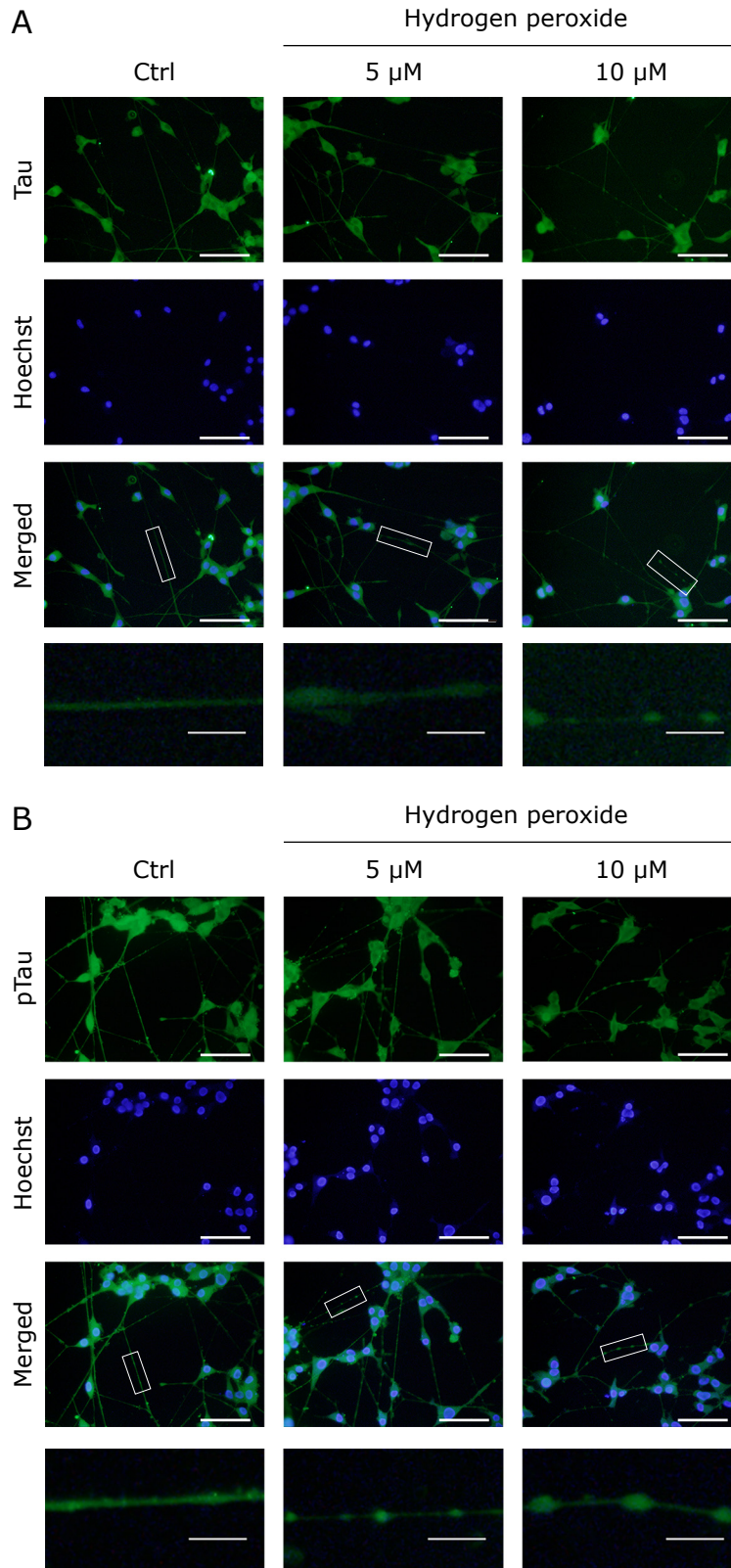


**Fig. 2.** (A, B) Confirmation of tau and pTau (green) presence (by immunostaining) and neurite degeneration in N1E-115 cells following exposure to hydrogen peroxide. Nuclei were counterstained with Hoechst 33258 (blue). Scale bars represent 100  $\mu$ m. Images are representative of three independent experiments. The neurites outlined by the white rectangle in the merged images are shown at higher magnification in the fourth row of each panel. Scale bars of the magnified neurites represent 20  $\mu$ m. Ctrl, control. See color figure in the on-line version.

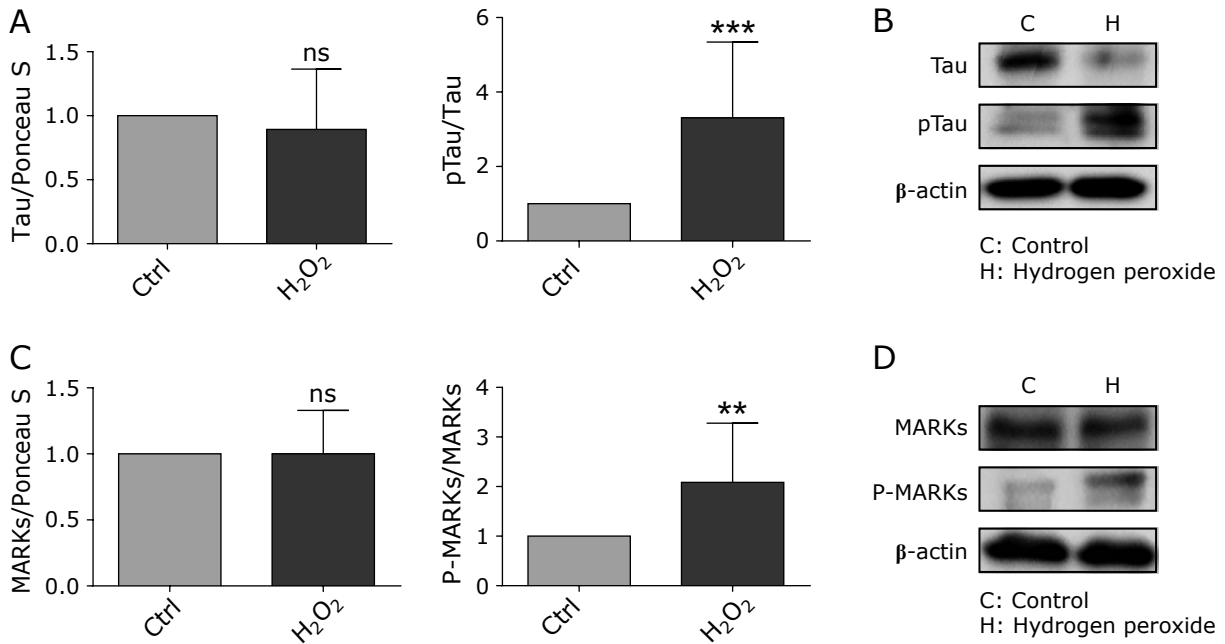


**Fig. 3.** (A, C) Changes in tau and MARK protein levels in N1E-115 cells following exposure to hydrogen peroxide. Gray columns indicate control (Ctrl) samples ( $n = 12$ ), and black columns indicate samples exposed to 5  $\mu\text{M}$  hydrogen peroxide ( $n = 12$ ). The ratios of each protein band intensity to Ponceau 5 staining intensity are shown; the ratios of the control samples were defined as 1. For both tau and the MARKs, the level of the phosphorylated form was divided by that of the unphosphorylated form of the same protein. Data are plotted as mean + SD of three independent experiments. \*\* $p < 0.01$ , \*\*\* $p < 0.001$  (two-tailed non-paired Student's  $t$  test, compared to the respective control). ns, not significant ( $p \geq 0.05$ ).  $\beta$ -Actin was used to visually confirm similar amounts of protein were loaded. Images of Western blots probed for the indicated protein are shown in (B) and (D).

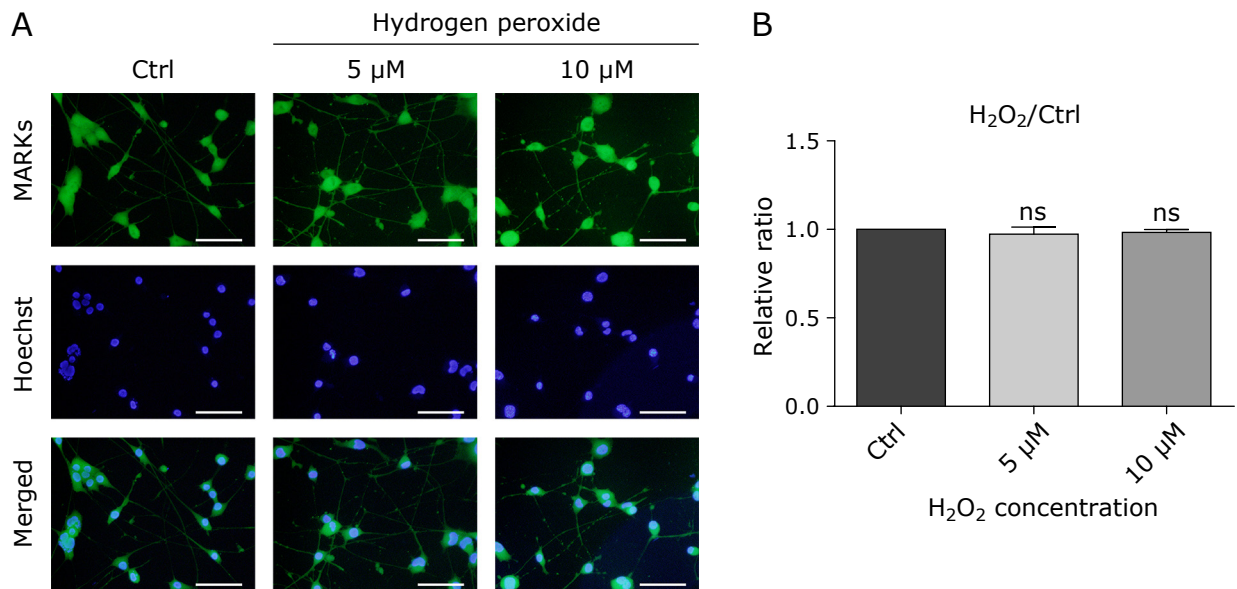


**Fig. 4.** (A) Confirmation of MARK (green) protein presence (by immunostaining) and neurite degeneration in N1E-115 cells following exposure to hydrogen peroxide. (B) Scale bars are 100  $\mu\text{m}$ . In the graph, the brightness relative ratio of hydrogen peroxide-exposed samples and control (Ctrl) are plotted; values were normalized to those in the control samples, such that the ratios of the control sample were defined as 1. Specifically, in each experiment, five cells were randomly selected and their brightnesses were measured using ImageJ software. Data are plotted as mean + SD of at least three independent experiments. ns, not significant ( $p \geq 0.05$ ; two-tailed one-way ANOVA with post hoc Tukey–Kramer's tests, compared to control). The micrographs are representative images. See color figure in the on-line version.

stress environment, we used hydrogen peroxide. In previous work with other types of cells, we confirmed that exposure to a low concentration of hydrogen peroxide induces neurite degener-

ation.<sup>(36,37)</sup> Nonetheless, it was essential to demonstrate that early changes occurred under oxidative stress, presumably reflecting physiologically relevant concentrations of hydrogen peroxide

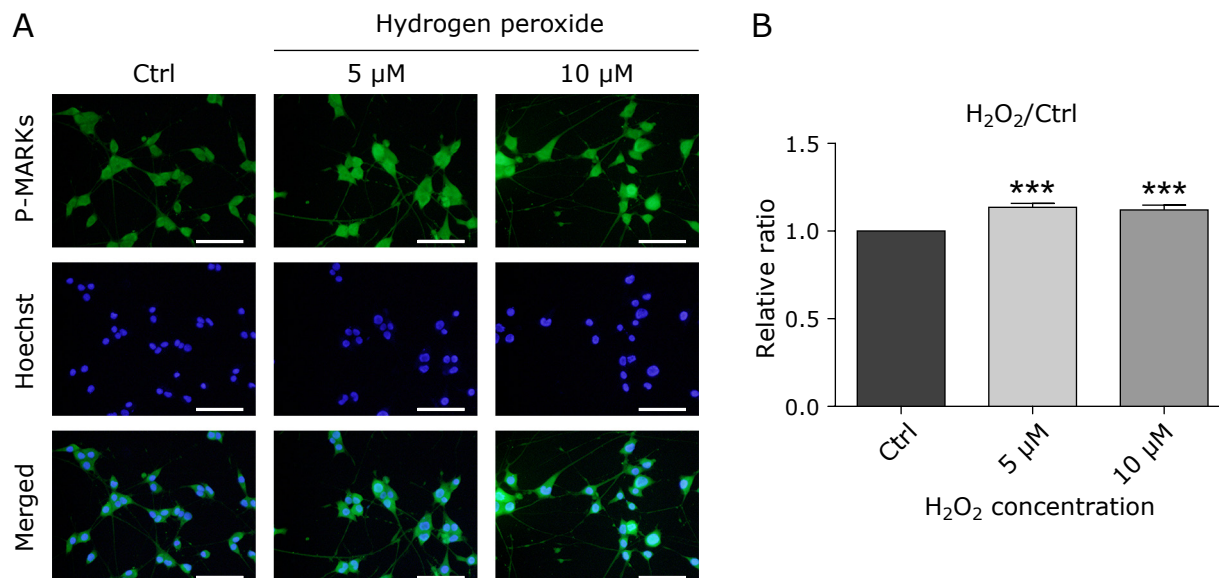


**Fig. 5.** (A, B) Confirmation of pMARK (green) protein levels (by immunostaining) and neurite degeneration in non-dividing N1E-115 cells following exposure to hydrogen peroxide. Details are identical to those in Fig. 4. Data are plotted as mean + SD of at least three independent experiments. \*\*\* $p < 0.001$  (two-tailed one-way ANOVA with post hoc Tukey–Kramer’s tests, compared to the control). See color figure in the on-line version.

that occur in living tissues. Before starting this study, we optimized the hydrogen peroxide concentration at which to expose N1E-115, in studies using both immunocytochemical and Western blotting analyses. Notably, exposure of N1E-115 cells to hydrogen peroxide induced cell death in an apparently concentration-dependent manner (Fig. 1C). Cell death exceeding 50% was observed following exposure to 20 μM hydrogen peroxide. At hydrogen peroxide concentrations lower than 10 μM, cell death was largely avoided. However, neurite degeneration was observed at hydrogen peroxide concentrations exceeding 1 μM. Neurite degeneration is an important marker for this study, since the purpose of this study was to reproduce the early pathology of AD in cultured cells. Mean cell survival rates of approximately 80 and 80% were confirmed in N1E-115 cells exposed to 5 and 10 μM hydrogen peroxide (respectively). Therefore, we selected 5 and 10 μM hydrogen peroxide as the optimal concentrations for subsequent experiments. Specifically, morphological changes (beading) were observed in the neurites of N1E-115 cells following exposure to hydrogen peroxide at these concentrations (Fig. 1B). Beading is a major sign of neurite degeneration, which has been identified as occurring in the early stages of several neurodegenerative diseases such as dementia, AD, and multiple sclerosis.

Nevertheless, for undetermined reasons, cells growing in 35-mm dishes did not withstand the concentrations of hydrogen peroxide previously mentioned. Hence, the optimal concentration could not be applied to samples intended for Western blotting. As we mentioned above, optimization of hydrogen peroxide concentration was performed using 24-well plates. Notably, cells had to be grown to higher confluence (exceeding 80%) in dishes to permit collection of lysates with protein concentrations sufficient (typically, permitting loading of >20 μg/lane) for use in Western blotting. This higher confluence may have been the basis of the elevated cell death seen when dish-grown cells were exposed to 10 μM hydrogen peroxide. Therefore, we only used 5 μM hydrogen peroxide in cultures intended for use in Western blotting, in contrast to the 5 and 10 μM hydrogen peroxide concentrations used in cultures intended for immunocytochemical analysis.

**N1E-115 is a suitable model for the study of the MARK-Tau signaling pathway.** In a previous study, we confirmed that N1E-115 cells, which are derived from a mouse neuroblastoma, have the properties of short growth cycle, low cost, and ease of imaging, as well as the ability to generate elongated neurites via exposure to DMSO (without the use of nerve growth factor). In addition, N1E-115 cells have been shown to produce tau phosphorylated at Ser404 in response to oxidative stress, as shown by Western blotting.<sup>(38)</sup> For these reasons, N1E-115 cells are a suitable model for studying tau pathology. In the present study, we confirmed using Western blotting that N1E-115 cells produce tau phosphorylated at Ser262. However, to the best of our knowledge, no information is available about the expression of MARKs in N1E-115 cells. N1E-115 cells usually are used for studies of neural signaling pathways and function, especially regarding the central nervous system.<sup>(39,40)</sup> Additionally, given that these cells are derived from a common form of neural cancer, the line serves as a model for studying proteins or genes related to cancer.<sup>(41,42)</sup> MARKs activity is regulated by LKB1, and various researchers have suggested that LKB1 may serve as an inhibitor or promoter of cancer.<sup>(43,44)</sup> The aim of the present study was to assess the relationship between MARKs and tau hyperphosphorylation under oxidative stress. Additionally, the N1E-115 line is derived from neural cancer, and we assume that N1E-115 cells also can produce proteins related to cancer, whose effects may be mediated via LKB1 and downstream MARKs. The results of the present study confirmed the expression of MARKs in N1E-115 cells, demonstrating that N1E-115 is a suitable model for research on the MARK-tau signaling pathway in AD.

**Oxidative stress induces the accumulation of tau phosphorylated at Ser262, a process related to the activation of MARKs in the early stages of AD.** Hyperphosphorylated tau is a major component of NFTs, which are a hallmark of AD. Much research has suggested that tau pathology in neurodegeneration is associated with oxidative stress.<sup>(44)</sup> Accumulating evidence suggests that oxidative stress contributes to the development of NFTs in AD via acceleration of the polymerization of tau by oxidation of polyunsaturated fatty acids.<sup>(45,46)</sup> Moreover, p38 mitogen-activated protein kinase (MAPK), one of the kinases

shown to phosphorylate tau, has been shown to be activated by oxidative stress *in vitro*.<sup>(47)</sup> Those studies suggested that tau hyperphosphorylation renders tau more susceptible to PHF formation, leading in turn to NFTs. As we mentioned earlier, tau phosphorylated at Ser262 is an early pathological change that is thought to lead to subsequent abnormal accumulation of tau. We confirmed that the level of tau phosphorylated at Ser262 increases significantly following exposure to hydrogen peroxide, and the levels of MARKs also significantly increase in hydrogen peroxide-treated cells compared to the controls. In addition, some researchers have already demonstrated that the reduction of the phosphorylation of tau is relative to treatment with multiple MARK4 inhibitors and it clues the MARK4 inhibition as tau is a substrate for MARK4.<sup>(48)</sup> It can be considered strong evidence to explain the relevance between tau hyperphosphorylation and the MARKs phosphorylation. Taken together, the evidence suggests that MARKs activation may play an important role in the initial changes in this experimental model of AD. It is possible that tau pathology is induced in response to oxidative stress conditions. MARKs activation may lead to tau hyperphosphorylation at Ser262 as the initially occurring pathology, along with the activation of other tau kinases (such as p38) in response to oxidative stress; tau phosphorylation then might guide a series of changes ultimately leading to the formation of NFTs. Meanwhile, many studies have demonstrated the relationship between oxidative stress and tau pathology, including the potential therapeutic role of antioxidants, effects that have been shown both in a *Drosophila* model of human tauopathy (tau R406W)<sup>(49)</sup> and in transgenic AD (Tg2576) mice.<sup>(50)</sup>

Those previous studies confirmed that overexpression of some antioxidant enzymes, such as mitochondrial superoxide dismutase (SOD2), or exposure to vitamin E decreases tau-induced neuronal death, while a lack of SOD2 or a decrease in the cytoplasmic SOD paralog (SOD1) induces tau phosphorylation.<sup>(49–51)</sup> This evidence suggests that antioxidative effects may prevent tau phosphorylation at Ser262 in the early stages of AD by preventing the activation of MARKs and thereby impeding AD-associated deterioration of brain function. MARKs may be useful as potential drug targets for AD. However, further studies will be required to fully clarify the mechanism of oxidative stress in tau pathology via regulation by MARKs.

**MARKs isoforms relevant to AD.** In this study, we confirmed (using mixed anti-pMARK antibodies [MARK4 (phospho T214) + MARK2 (phospho T208) + MARK3 (phospho T234) + MARK1 (phospho T215)]) that pMARKs protein levels increase following exposure to hydrogen peroxide, leading to tau hyperphosphorylation at Ser262. However, we could not distinguish which MARKs protein was activated or which paralog had the most profound effect on tau phosphorylation at Ser262. Some research has suggested that the subcellular localization of MARK4 is distinct from that of the other MARK isoforms.<sup>(21,52)</sup> For example, several studies have shown that MARK4 localizes with centrosomes and microtubules. Notably, MARK4, which is expressed as two isoforms (long (MARK4L) and short (MARK4S), differing by the presence [in the corresponding transcripts] of an additional exon), shows distinct affinities for the centrosome.<sup>(53,54)</sup> Several lines of research suggest that these two isoforms are differentially expressed in human tissues. MARK4S is expressed in normal brain tissue and neurons, indicating that MARK4S may contribute to neuronal differentiation. On the other hand, MARK4L is upregulated in cells such as hepatocarcinoma cell lines and neural progenitor cells, suggesting that MARK4L may play a crucial role in cell proliferation.<sup>(55–57)</sup> Separately, MARK4 has been shown to interact with centriolar proteins during the G0/G1 phase of mitotic division.<sup>(58,59)</sup> Moreover, MARK4 overexpression in rat hippocampus after mitosis

has been shown to induce tau hyperphosphorylation.<sup>(24)</sup> These results may provide a possible explanation for our results. In our studies, we found that the levels of pMARKs, as assessed by Western blotting and relative intensity by immunocytochemistry, are higher in hydrogen peroxide treated cells compare to the untreated cells. (Fig. 5B). Taking our data and several previous research together, it is possible that tau phosphorylation may be more closely related to MARK4 activation than to that of other MARK proteins. However, MARK4 protein levels were not assessed in this study, further experiments are necessary.

In conclusion, we confirmed that MARK phosphorylation correlates with tau hyperphosphorylation at Ser262, a site that is essential for the maintenance of microtubule stability and is the initial phosphorylation site in AD pathogenesis. These results indicate that MARKs inhibitors might serve as tools for the treatment of AD.

## Author Contributions

Conceptualization, KF; Data curation, YC, YL, and KF; Formal analysis, KF; Investigation, YC, YL, and KF; Project administration, KF; Writing, review and editing, YL and KF; All other contributions to the research, KF.

## Acknowledgments

We thank Mr. Mitsuru Wakuzawa for valuable technical advice on cell culture experiments.

## Funding

This research received no external private funding.

## Abbreviations

AD	Alzheimer's disease
BSA	bovine serum albumin
DMSO	dimethyl sulfoxide
ECL	enhanced chemiluminescence
EHS	Engelbreth-Holm-Swarm
FBS	fetal bovine serum
GSK3β	glycogen synthase kinase 3β
KIN1	protein kinase in <i>S. cerevisiae</i>
LKB1	liver kinase B1
MAP	microtubule-associated protein
MARK	microtubule affinity-regulating kinase
MARKK	microtubule affinity-regulating kinases kinase
MS	multiple sclerosis
NFT	neurofibrillary tangle
PAR-1	proteinase-activated receptor 1
PBS	phosphate-buffered saline
PEI	polyethyleneimine
PFA	paraformaldehyde
PHF	paired helical filament
RNS	reactive nitrogen species
ROS	reactive oxygen species
SDS	sodium dodecyl sulfate
SOD1	cytoplasmic superoxide dismutase
SOD2	mitochondrial superoxide dismutase
TBS	Tris-HCl-buffered saline
T-loop	activation loop

## Conflict of Interest

No potential conflicts of interest were disclosed.

## References

- 1 Harman D. Free radical theory of aging: history. *Exs* 1992; **62**: 1–10.
- 2 Willcox JK, Ash SL, Catignani GL. Antioxidants and prevention of chronic disease. *Crit Rev Food Sci Nutr* 2004; **44**: 275–295.
- 3 Genestra M. Oxy radicals, redox-sensitive signalling cascades and antioxidants. *Cell Signal* 2007; **19**: 1807–1819.
- 4 Sies H, Chance B. The steady state level of catalase compound I in isolated hemoglobin-free perfused rat liver. *FEBS Lett* 1970; **11**: 172–176.
- 5 Valko M, Morris H, Cronin MT. Metals, toxicity and oxidative stress. *Curr Med Chem* 2005; **12**: 1161–1208.
- 6 Chen Z, Zhong C. Oxidative stress in Alzheimer's disease. *Neurosci Bull* 2014; **30**: 271–281.
- 7 Fukui K, Okihiro S, Ohfuchi Y, *et al.* Proteomic study on neurite responses to oxidative stress: search for differentially expressed proteins in isolated neurites of N1E-115 cells. *J Clin Biochem Nutr* 2019; **64**: 36–44.
- 8 Spires-Jones TL, Hyman BT. The intersection of amyloid beta and tau at synapses in Alzheimer's disease. *Neuron* 2014; **82**: 756–771.
- 9 Golde TE. Open questions for Alzheimer's disease immunotherapy. *Alzheimers Res Ther* 2014; **6**: 3.
- 10 Sarazin M, Dorothée G, de Souza LC, Aucouturier P. Immunotherapy in Alzheimer's disease: do we have all the pieces of the puzzle? *Biol Psychiatry* 2013; **74**: 329–332.
- 11 Braak H, Braak E. Evolution of the neuropathology of Alzheimer's disease. *Acta Neurol Scand Suppl* 1996; **165**: 3–12.
- 12 Duan AR, Jonasson EM, Alberico EO, *et al.* Interactions between tau and different conformations of tubulin: implications for tau function and mechanism. *J Mol Biol* 2017; **429**: 1424–1438.
- 13 Bloom GS. Amyloid- $\beta$  and tau: the trigger and bullet in Alzheimer disease pathogenesis. *JAMA Neurol* 2014; **71**: 505–508.
- 14 Callahan LM, Vaules WA, Coleman PD. Progressive reduction of synaptophysin message in single neurons in Alzheimer disease. *J Neuropathol Exp Neurol* 2002; **61**: 384–395.
- 15 Bear MF, Connors BW, Paradiso MA. *Neuroscience: Exploring the Brain*. Burlington: Jones & Bartlett Learning, 2020.
- 16 Liu F, Li B, Tung EJ, Grundke-Iqbal I, Iqbal K, Gong CX. Site-specific effects of tau phosphorylation on its microtubule assembly activity and self-aggregation. *Eur J Neurosci* 2007; **26**: 3429–3436.
- 17 Drewes G, Ebnet A, Preuss U, Mandelkow EM, Mandelkow E. MARK, a novel family of protein kinases that phosphorylate microtubule-associated proteins and trigger microtubule disruption. *Cell* 1997; **89**: 297–308.
- 18 Matenia D, Mandelkow EM. The tau of MARK: a polarized view of the cytoskeleton. *Trends Biochem Sci* 2009; **34**: 332–342.
- 19 Timm T, Balusamy K, Li X, Biernat J, Mandelkow E, Mandelkow EM. Glycogen synthase kinase (GSK) 3 $\beta$  directly phosphorylates Serine 212 in the regulatory loop and inhibits microtubule affinity-regulating kinase (MARK) 2. *J Biol Chem* 2008; **283**: 18873–18882.
- 20 Espinosa L, Navarro E. Human serine/threonine protein kinase EMK1: genomic structure and cDNA cloning of isoforms produced by alternative splicing. *Cytogenet Cell Genet* 1998; **81**: 278–282.
- 21 Trinczek B, Brajenovic M, Ebnet A, Drewes G. MARK4 is a novel microtubule-associated proteins/microtubule affinity-regulating kinase that binds to the cellular microtubule network and to centrosomes. *J Biol Chem* 2004; **279**: 5915–5923.
- 22 Lasagna-Reeves CA, de Haro M, Hao S, *et al.* Reduction of Nuak1 decreases tau and reverses phenotypes in a tauopathy mouse model. *Neuron* 2016; **92**: 407–418.
- 23 Augustinack JC, Schneider A, Mandelkow EM, Hyman BT. Specific tau phosphorylation sites correlate with severity of neuronal cytopathology in Alzheimer's disease. *Acta Neuropathol* 2002; **103**: 26–35.
- 24 Yu W, Polepalli J, Wagh D, Rajadas J, Malenka R, Lu B. A critical role for the PAR-1/MARK-tau axis in mediating the toxic effects of A $\beta$  on synapses and dendritic spines. *Hum Mol Genet* 2012; **21**: 1384–1390.
- 25 Zempel H, Thies E, Mandelkow E, Mandelkow EM. A $\beta$  oligomers cause localized Ca<sup>2+</sup> elevation, missorting of endogenous Tau into dendrites, Tau phosphorylation, and destruction of microtubules and spines. *J Neurosci* 2010; **30**: 11938–11950.
- 26 Ando K, Maruko-Otake A, Ohtake Y, Hayashishita M, Sekiya M, Iijima KM. Stabilization of microtubule-unbound tau via tau phosphorylation at Ser262/356 by Par-1/MARK contributes to augmentation of AD-related phosphorylation and A $\beta$ 42-induced tau toxicity. *PLoS Genet* 2016; **12**: e1005917.
- 27 Ando K, Oka M, Ohtake Y, *et al.* Tau phosphorylation at Alzheimer's disease-related Ser356 contributes to tau stabilization when PAR-1/MARK activity is elevated. *Biochem Biophys Res Commun* 2016; **478**: 929–934.
- 28 Alonso AD, Di Clerico J, Li B, *et al.* Phosphorylation of tau at Thr212, Thr231, and Ser262 combined causes neurodegeneration. *J Biol Chem* 2010; **285**: 30851–30860.
- 29 Iijima-Ando K, Sekiya M, Maruko-Otake A, *et al.* Loss of axonal mitochondria promotes tau-mediated neurodegeneration and Alzheimer's disease-related tau phosphorylation via PAR-1. *PLoS Genet* 2012; **8**: e1002918.
- 30 Iijima K, Gatt A, Iijima-Ando K. Tau Ser262 phosphorylation is critical for A $\beta$ 42-induced tau toxicity in a transgenic Drosophila model of Alzheimer's disease. *Hum Mol Genet* 2010; **19**: 2947–2957.
- 31 Hynes RO. Integrins: versatility, modulation, and signaling in cell adhesion. *Cell* 1992; **69**: 11–25.
- 32 Turner DC, Flier LA. Receptor-mediated active adhesion to the substratum is required for neurite outgrowth. *Dev Neurosci* 1989; **11**: 300–312.
- 33 Sarner S, Kozma R, Ahmed S, Lim L. Phosphatidylinositol 3-kinase, Cdc42, and Rac1 act downstream of Ras in integrin-dependent neurite outgrowth in N1E-115 neuroblastoma cells. *Mol Cell Biol* 2000; **20**: 158–172.
- 34 Pham-Huy LA, He H, Pham-Huy C. Free radicals, antioxidants in disease and health. *Int J Biomed Sci* 2008; **4**: 89–96.
- 35 Wood C. *Free Radicals in Biology and Medicine. Third Edition: Barry Halliwell and John M.C. Gutteridge, Oxford University Press. ISBN 1-29-850044-0/45-0. H/B £75.00, P/B £34.95. Int J Biochem Cell Biol* 1999; 1454.
- 36 Fukui K, Ushiki K, Takatsu H, Koike T, Urano S. Tocotrienols prevent hydrogen peroxide-induced axon and dendrite degeneration in cerebellar granule cells. *Free Radic Res* 2012; **46**: 184–193.
- 37 Fukui K, Takatsu H, Koike T, Urano S. Hydrogen peroxide induces neurite degeneration: prevention by tocotrienols. *Free Radic Res* 2011; **45**: 681–691.
- 38 Benítez-King G, Ortíz-López L, Jiménez-Rubio G, Ramírez-Rodríguez G. Haloperidol causes cytoskeletal collapse in N1E-115 cells through tau hyperphosphorylation induced by oxidative stress: implications for neurodevelopment. *Eur J Pharmacol* 2010; **644**: 24–31.
- 39 Shastry P, Basu A, Rajadhyaksha MS. Neuroblastoma cell lines—a versatile *in vitro* model in neurobiology. *Int J Neurosci* 2001; **108**: 109–126.
- 40 Marler KJ, Kozma R, Ahmed S, Dong JM, Hall C, Lim L. Outgrowth of neurites from N1E-115 neuroblastoma cells is prevented on repulsive substrates through the action of PAK. *Mol Cell Biol* 2005; **25**: 5226–5241.
- 41 Kisaalita WS, Bowen JM. Effect of culture age on the susceptibility of differentiating neuroblastoma cells to retinoid cytotoxicity. *Biotechnol Bioeng* 1996; **50**: 580–586.
- 42 Kisaalita WS, Bowen JM. Effect of medium serum concentration on N1E-115 neuroblastoma membrane potential development. *In Vitro Cell Dev Biol Anim* 1997; **33**: 152–155.
- 43 Li TT, Zhu HB. LKB1 and cancer: the dual role of metabolic regulation. *Biomed Pharmacother* 2020; **132**: 110872.
- 44 Ciccarese F, Zulato E, Indraccolo S. LKB1/AMPK pathway and drug response in cancer: a therapeutic perspective. *Oxid Med Cell Longev* 2019; **2019**: 8730816.
- 45 Iqbal K, Alonso AC, Gong CX, *et al.* Mechanisms of neurofibrillary degeneration and the formation of neurofibrillary tangles. *J Neural Transm Suppl* 1998; **53**: 169–180.
- 46 Gamblin TC, King ME, Kuret J, Berry RW, Binder LI. Oxidative regulation of fatty acid-induced tau polymerization. *Biochemistry* 2000; **39**: 14203–14210.
- 47 Schweers O, Mandelkow EM, Biernat J, Mandelkow E. Oxidation of cysteine-322 in the repeat domain of microtubule-associated protein tau controls the *in vitro* assembly of paired helical filaments. *Proc Natl Acad Sci U S A* 1995; **92**: 8463–8467.
- 48 Voura M, Khan P, Thysiadis S, *et al.* Probing the inhibition of microtubule affinity regulating kinase 4 by *N*-substituted acridones. *Sci Rep* 2019; **9**: 1676.
- 49 Dias-Santagata D, Fulga TA, Duttaroy A, Feany MB. Oxidative stress mediates tau-induced neurodegeneration in Drosophila. *J Clin Invest* 2007; **117**: 236–245.
- 50 Stamer K, Vogel R, Thies E, Mandelkow E, Mandelkow EM. Tau blocks traffic of organelles, neurofilaments, and APP vesicles in neurons and

- enhances oxidative stress. *J Cell Biol* 2002; **156**: 1051–1063.
- 51 Goedert M, Hasegawa M, Jakes R, Lawler S, Cuenda A, Cohen P. Phosphorylation of microtubule-associated protein tau by stress-activated protein kinases. *FEBS Lett* 1997; **409**: 57–62.
- 52 Melov S, Adlard PA, Morten K, *et al.* Mitochondrial oxidative stress causes hyperphosphorylation of tau. *PLoS One* 2007; **2**: e536.
- 53 Rovina D, Fontana L, Monti L, *et al.* Microtubule-associated protein/microtubule affinity-regulating kinase 4 (MARK4) plays a role in cell cycle progression and cytoskeletal dynamics. *Eur J Cell Biol* 2014; **93**: 355–365.
- 54 Magnani I, Novielli C, Bellini M, Roversi G, Bello L, Larizza L. Multiple localization of endogenous MARK4L protein in human glioma. *Cell Oncol* 2009; **31**: 357–370.
- 55 Beghini A, Magnani I, Roversi G, *et al.* The neural progenitor-restricted isoform of the MARK4 gene in 19q13.2 is upregulated in human gliomas and overexpressed in a subset of glioblastoma cell lines. *Oncogene* 2003; **22**: 2581–2591.
- 56 Kato T, Satoh S, Okabe H, *et al.* Isolation of a novel human gene, MARKL1, homologous to MARK3 and its involvement in hepatocellular carcinogenesis. *Neoplasia* 2001; **3**: 4–9.
- 57 Moroni RF, De Biasi S, Colapietro P, Larizza L, Beghini A. Distinct expression pattern of microtubule-associated protein/microtubule affinity-regulating kinase 4 in differentiated neurons. *Neuroscience* 2006; **143**: 83–94.
- 58 Magnani I, Novielli C, Fontana L, *et al.* Differential signature of the centrosomal MARK4 isoforms in glioma. *Anal Cell Pathol (Amst)* 2011; **34**: 319–338.
- 59 Kuhns S, Schmidt KN, Reymann J, *et al.* The microtubule affinity regulating kinase MARK4 promotes axoneme extension during early ciliogenesis. *J Cell Biol* 2013; **200**: 505–522.



This is an open access article distributed under the terms of the Creative Commons Attribution-NonCommercial-NoDerivatives License (<http://creativecommons.org/licenses/by-nc-nd/4.0/>).

---